



**Inclusive Production of  $\eta'(958)$  and  $f_0(975)$  Mesons  
in the  $\Upsilon$  Energy Region**

The ARGUS Collaboration

ISSN 0418-9833

**NOTKESTRASSE 85 · D - 2000 HAMBURG 52**

**DESY behält sich alle Rechte für den Fall der Schutzrechtserteilung und für die wirtschaftliche Verwertung der in diesem Bericht enthaltenen Informationen vor.**

**DESY reserves all rights for commercial use of information included in this report, especially in case of filing application for or grant of patents.**

To be sure that your preprints are promptly included in the  
**HIGH ENERGY PHYSICS INDEX,**  
send them to (if possible by air mail):

**DESY  
Bibliothek  
Notkestraße 85  
W-2000 Hamburg 52  
Germany**

**DESY-IfH  
Bibliothek  
Platanenallee 6  
O-1615 Zeuthen  
Germany**

## Inclusive Production of $\eta'(958)$ and $f_0(975)$ Mesons in the $\Upsilon$ Energy Region

The ARGUS Collaboration

H. Albrecht, H. Ehrlichmann, T. Hamacher, R. P. Hofmann, T. Kirchhoff, A. Nau,  
S. Nowak<sup>1</sup>, H. Schröder, H. D. Schulz, M. Walter<sup>1</sup>, R. Würth  
DESY, Hamburg, Germany

R. D. Appuhn, C. Hast, H. Kolanoski, A. Kosche, A. Lange, A. Lindner, R. Mankel,  
M. Schieber, T. Siegmund, B. Spaan, H. Thurn, D. Töpfer, A. Walther, D. Wegener,  
A. Zimmermann  
Institut für Physik<sup>2</sup>, Universität Dortmund, Germany

M. Bittner, P. Eckstein  
Institut für Kern- und Teilchenphysik<sup>3</sup>, Technische Universität Dresden, Germany

M. Paulini, K. Reim, H. Wegener  
Physikalisches Institut<sup>4</sup>, Universität Erlangen-Nürnberg, Germany

R. Mundt, T. Oest, R. Reiner, W. Schmidt-Parzefall  
II. Institut für Experimentalphysik, Universität Hamburg, Germany

W. Funk, J. Stiewe, S. Werner

Institut für Hochenergiephysik<sup>5</sup>, Universität Heidelberg, Germany

K. Ehret, W. Hofmann, A. Hüpper, S. Khan, K. T. Knöpfe, M. Seeger, J. Spengler  
Max-Planck-Institut für Kernphysik, Heidelberg, Germany

D. I. Britton<sup>6</sup>, C. E. K. Charlesworth<sup>7</sup>, K. W. Edwards<sup>8</sup>, E. R. F. Hyatt<sup>6</sup>, H. Kapitza<sup>8</sup>,  
P. Krieger<sup>7</sup>, D. B. MacFarlane<sup>6</sup>, P. M. Patel<sup>6</sup>, J. D. Prentice<sup>7</sup>, P. R. B. Saull<sup>6</sup>,  
K. Tzamaridouaki<sup>6</sup>, R. G. Van de Water<sup>7</sup>, T.-S. Yoon<sup>7</sup>  
Institute of Particle Physics<sup>10</sup>, Canada

D. Reßing, M. Schmidtler, M. Schneider, K. R. Schubert, K. Strahl, R. Waldi, S. Weseler  
Institut für Experimentelle Kernphysik<sup>11</sup>, Universität Karlsruhe, Germany

G. Kernel, P. Križan, E. Križnič, T. Podobnik, T. Živko  
Institut J. Stefan and Oddetek za fiziko<sup>12</sup>, Univerza v Ljubljani, Ljubljana, Slovenia

V. Balagura, I. Belyaev, S. Chechelnitzky, M. Danilov, A. Droutskoy, Yu. Gershtein,  
A. Golutvin, I. Gorelov, G. Kostina, V. Lubimov, P. Pakhlov, F. Ratnikov, S. Semenov,  
V. Shibaev, V. Soloshenko, I. Tichomirow, Yu. Zaitsev  
Institute of Theoretical and Experimental Physics, Moscow, Russia

<sup>1</sup> DESY, IfH Zeuthen.

<sup>2</sup> Supported by the German Bundesministerium für Forschung und Technologie, under contract number 054DO51P.

<sup>3</sup> Supported by the German Bundesministerium für Forschung und Technologie, under contract number 055DD11P.

<sup>4</sup> Supported by the German Bundesministerium für Forschung und Technologie, under contract number 054ER12P.

<sup>5</sup> Supported by the German Bundesministerium für Forschung und Technologie, under contract number 055HD21P.

<sup>6</sup> McGill University, Montreal, Quebec, Canada.

<sup>7</sup> University of Toronto, Toronto, Ontario, Canada.

<sup>8</sup> Carleton University, Ottawa, Ontario, Canada.

<sup>9</sup> Supported in part by the Walter C. Sumner Foundation.

<sup>10</sup> Supported by the Natural Sciences and Engineering Research Council, Canada.

<sup>11</sup> Supported by the German Bundesministerium für Forschung und Technologie, under contract number 054KA17P.

<sup>12</sup> Supported by the Department of Science and Technology of the Republic of Slovenia and the Internationales Büro KfA, Jülich.

### Abstract

The inclusive production cross sections of  $\eta'(958)$  and  $f_0(975)$  mesons are measured in  $e^+e^-$  annihilation in the nonresonant continuum around  $\sqrt{s} = 10$  GeV and in decays of the  $\Upsilon$  resonances using the ARGUS detector. For  $\eta'(958)$  mesons, a production ratio of  $\eta'(958)/\eta_{dir} = 0.35 \pm 0.24$ , with  $\eta_{dir} = \eta - BR(\eta' \rightarrow \eta X) \cdot \eta'$ , is determined in direct  $\Upsilon(1S)$  decays, which can be partially explained by the pseudoscalar singlet/octet mixing. For  $f_0(975)$  production, we obtain a production ratio of  $f_0(975)/\rho(770)^0 = 0.117 \pm 0.030$  in direct  $\Upsilon(1S)$  decays. In its production features, the  $f_0(975)$  behaves like an ordinary meson, though a  $K\bar{K}$  molecule nature cannot be excluded. The substantial production yield of the  $f_0(975)$  meson demonstrates the important effect of feeddown from mesons beyond the basic multiplets on pseudoscalar and vector meson production.

## 1 Introduction

The understanding of hadron formation in jet fragmentation has been a challenge for almost 20 years. While the small momentum transfers involved in these transitions will keep this part of physics inaccessible to pure QCD at least for some time in the future, the need of coping with fragmenting systems has lead to phenomenological approaches describing the breakup of a colour field into hadrons. It is now a widely used concept that the probability of a certain hadron to form in the hadronization step is mainly determined by its quark content. For example, for each strange valence quark in the meson, its production rate is attenuated by a certain factor,  $s/u$ , relative to those mesons containing a light  $u$ - or  $d$ -quark in the same place. This approach, which was first used by Feynman and Field [1] and later incorporated into the Lund models [2] proved to be quite successful in describing the relative production rates of strange mesons and baryons [3, 4]. With additional corrections from spin-spin interaction and the shapes of meson wave functions, one can hope to obtain a basically simple, universal picture. It is of particular importance to check how other quantum numbers, as isospin, or mixing of different  $SU(3)$  multiplet states influence the production probability.

This can be sensitively tested by studying the production of the  $\eta'(958)$  meson, which is the least thoroughly investigated light pseudoscalar meson. The  $\eta'(958)$  and  $\eta$  mesons feature similar quantum numbers but remarkably different masses and form therefore an ideal system to look for explicit mass effects in hadronization. This can be studied by comparing with predictions of different model approaches: the Lund model [2], which incorporates a strangeness suppression, but no explicit mass suppression, and the UCLA model [5], which is a derivative of the Lund model as far as fragmentation is concerned, but incorporates mass dependent probabilities for the creation of different hadron species. For most pseudoscalar and vector mesons, the Lund and UCLA model predictions do not differ strongly from each other, since strangeness in a hadron means usually more mass. The  $\eta'(958)/\eta$  system is perhaps the best place to look for such subtle differences, since here the mass difference of mesons with related quark content is particularly large. However, conclusions from  $\eta'(958)$  and  $\eta$  production in  $q\bar{q}$  fragmentation, prevalent in nonresonant  $e^+e^-$  continuum or in hadronic  $Z^0$  decays, are hindered by the fact that the inclusive branching ratios of charm and beauty hadrons into these mesons are not yet known with adequate precision. An elegant way to overcome this problem is opened through the study of direct  $\Upsilon(1S)$  decays, which proceed mainly through a three-gluon system so that charm production is suppressed [6].

A second crucial ingredient in a wholesome picture of hadronization is the role of mesons with non-zero angular momentum between the quarks. Their production is not only of interest with regard to its own dynamics. The  $L \neq 0$  states decay finally into lighter mesons without angular momentum and can be reckoned to contribute considerably to the pseudoscalar and vector meson yields. Thus, a complete understanding of light meson production is impossible without knowledge about  $L \neq 0$  mesons. In this paper we present the first study of  $f_0(975)$  production in the  $\Upsilon$  energy region, which can shed light on these basic questions.

## 2 Data analysis

The data used for this analysis have been obtained with the ARGUS detector at the  $e^+e^-$  storage ring DORIS II. The ARGUS detector is a  $4\pi$  magnetic spectrometer which is in detail described elsewhere [7]. The data sample used for the  $\eta'(958)$  and  $f_0(975)$  analyses comprises integrated luminosities of  $32 \text{ pb}^{-1}$  on the  $\Upsilon(1S)$ ,  $38 \text{ pb}^{-1}$  on the  $\Upsilon(2S)$ ,  $244 \text{ pb}^{-1}$  on the  $\Upsilon(4S)$  resonances and  $104 \text{ pb}^{-1}$  in the surrounding continuum. Hadronic events were selected by requiring at least three charged tracks with either a common vertex or an energy deposition of at least  $1.7 \text{ GeV}$  in the shower counters. As described in reference [8], events with uneven momentum balance were discarded to reject remnants from beam-gas, beam-wall and two-photon interactions. Charged hadrons were identified by means of combined likelihoods calculated from the available specific energy loss ( $dE/dx$ ) and time-of-flight (ToF) measurements for all possible particle hypotheses. A specific hypothesis was accepted for a particle if the corresponding relative likelihood exceeded 1% [7]. For the charged pions in the  $f_0(975)$  analysis, the cut was placed at 10% in order to reduce background from combinations with misidentified particles. Only photons with an energy  $E_\gamma > 50 \text{ MeV}$  were considered.

The acceptance for the  $\eta'(958)$  and  $f_0(975)$  candidates was obtained by using model events passed through a full detector simulation and the regular reconstruction chain. Special care has been taken in correcting the continuum rates for radiation effects and in subtracting contributions from electromagnetic processes like nonresonant continuum and vacuum polarization  $e^+e^- \rightarrow \Upsilon \rightarrow q\bar{q}$  which accompany the direct decays at the  $\Upsilon$  resonance energies. After applying corrections for soft and hard photon radiation as well as QCD effects [9], lowest order cross sections were obtained which could be scaled proportional to  $1/s$ . The energy spectra of the  $f_0(975)$  were expressed in the form  $1/(\beta\sigma_{\text{tot}}^0) \cdot d\sigma^0/dz$ , where  $z = 2E/\sqrt{s}$  and  $\beta$  stands for the particle's velocity. Corrections for the distortion of the particle spectra caused by initial state photon radiation were calculated using the model Lund 6.3 [2], where the radiation tails of the quarkonia resonances were accounted for by appropriate weighting. The different particle acceptances on and off the resonances and with or without initial state radiation were calculated separately and included in the cross section scaling [9].

## 3 Extraction of $\eta'(958)$ Rates

The production of  $\eta'(958)$  mesons was studied using the  $\eta\pi^+\pi^-$  decay mode which features the best compromise of reconstruction efficiency, branching ratio and background. Before  $\eta$  candidates could be reconstructed in their  $\gamma\gamma$  decay mode, the dominant background from neutral pion decays had to be reduced. For all possible  $\gamma\gamma$  combinations with  $|m_{\pi^+\pi^-} - m_{\pi^0}| < 50 \text{ MeV}/c^2$  or  $|m_{\pi^+\pi^-} - m_{\pi^0}| < 2 \cdot \delta m_{\pi\gamma}$ , where  $m_{\pi^0}$  stands for the nominal  $\pi^0$  mass and  $\delta m_{\pi\gamma}$  for the  $\gamma\gamma$  mass resolution, both photons were discarded from further analysis [10, 11]. The surviving photons

were subjected to a more rigid energy cut of  $E_\gamma > 100 \text{ MeV}$ , since an investigation of random trigger events revealed remnants of non-beam-beam origin, like calorimeter noise, beam-gas and beam-wall interactions below this threshold. The  $\eta$  candidates were then selected by combining two photon candidates within  $70 \text{ MeV}/c^2$  and three standard deviations of the nominal  $\eta$  mass. Their energy and momentum were constrained to the nominal  $\eta$  mass, before combining them with two oppositely charged pion candidates to obtain an  $\eta'(958)$  candidate. Since the remaining background in the low momentum photons was still too large, an additional momentum cut of  $p_\eta > 1 \text{ GeV}/c$  had to be imposed on the  $\eta$  candidate in order to extract a signal.

The invariant  $\eta\pi^+\pi^-$  mass spectra in the four sets of data are shown in figs. 1a–d. All four mass spectra show distinct signals at the nominal  $\eta'(958)$  mass over a smooth background. The mass spectra were first fitted with a Gaussian parameterization with free parameters plus a 4<sup>th</sup> order polynomial background function. Since the fitted values of signal mass and width were in good agreement with those obtained from a Monte Carlo simulation based on the standard parameters [12], the subsequent rate extraction was performed with mass and width fixed to the simulated values. These fit results are superimposed in figs. 1a–d.

Since the abovementioned cut on the momentum of  $\eta$  candidates prevents the selection of slow  $\eta'(958)$  mesons, the total rates per event have to incorporate a correction factor for the fraction of  $\eta'(958)$  mesons producing a daughter  $\eta$  meson with  $p_\eta > 1 \text{ GeV}/c$ . With one exception, we used the momentum spectrum shape generated by the Lund model to calculate the corrections. The thorough and model independent study of vector meson production in the  $\Upsilon$  energy region has shown that this model reproduces rather well the shape of momentum spectra in the continuum, while its predicted spectrum is too soft in the three-gluon decays of the  $\Upsilon(1S)$  resonance [9]. This effect was uniformly observed for  $\rho(770)$ ,  $K^*(892)$  and  $\omega(783)$  mesons. The spectra were easily fitted with the function  $dN/dz \sim \beta e^{-az}$  [9]. The resulting exponential slope parameters  $a$  are summarized in table 1. It is evident that the spectra of all four mesons can be described by a common parameterization as given above with the average parameter  $a = 10.6$ . Since neither the shape of the spectrum nor the relation to the model prediction depends significantly on the type of meson, the discrepancy appears to lie in the development of the parton cascade for the three-gluon decay rather than in the final hadronization stage where the meson flavours are produced. This conclusion gains support from the measurement of the photon spectrum from the decay  $\Upsilon(1S) \rightarrow \gamma gg$  [13]. Since the shapes of the spectra appear rather universal among the vector mesons and independent of flavour content, and since the  $\eta'(958)$  lies in the same mass range, we use the same shape to extrapolate the  $\eta'(958)$  momentum spectrum on the  $\Upsilon(1S)$  resonance.

## 4 Discussion of $\eta'(958)$ Measurements

The resulting  $\eta'(958)$  rates per event are shown in table 2, in comparison to the rates generated in the Lund 7.2 and the UCLA model [5, 14]. The systematic errors quoted here do not include uncertainties from the extrapolation procedure, since this would complicate comparison with models. In the cases of best significance, the  $\Upsilon(1S)$  and continuum samples, we also give the  $\eta'(958)$  rates for  $z > 0.35$ , with  $z = E_\eta/E_{\text{Beam}}$ , which can be determined without extrapolation and bear thus less model dependence than the total rate.

In the  $\Upsilon(4S)$  data, the direct  $\eta'(958)$  rate observed after continuum subtraction is smaller than the statistical error, which is mainly introduced by the subtraction procedure. Since the  $\Upsilon(4S)$  decays into a pair of B mesons, one can expect the dominant offspring for  $\eta'(958)$  production to be  $D_s^+$  decays. With the measured branching ratios of  $B \rightarrow D_s^+ X$  [15] and

$D_s^+ \rightarrow \eta' \pi^+$  [16], one thus expects at least 0.015  $\eta'$  mesons per  $B\bar{B}$  event, which is in accord with the data.

In the direct  $\Upsilon(1S)$  and  $\Upsilon(2S)$  decays, as well as in the continuum, the observed  $\eta'(958)$  rate emerges considerably lower than calculated in the Lund model. In order to check if the model disagreement is introduced by the extrapolation procedure, the  $\eta'(958)$  signal in the  $\Upsilon(1S)$  data was also extrapolated with the spectrum shape from Lund 7.2, which yields  $n_{\eta'} = 0.15 \pm 0.04 \pm 0.03$ , still in clear disaccord with the model value. The 36% change in the total  $\eta'(958)$  rate in direct  $\Upsilon(1S)$  decays might serve as a crude estimate of the systematic error introduced by the extrapolation. Also given in table 2 is the prediction of the UCLA model [5, 14], which incorporates a directly hadron mass dependent suppression of heavy particles in the hadronization step. At present, the latter model gives no prediction for  $\Upsilon$  decays [14]. For continuum events, the model gives a smaller  $\eta'(958)$  rate than the Lund model, but still larger than the measured value.

It is interesting to compare the  $\eta'(958)$  production rate to that of the  $\eta$  meson, its closest relative. To correct for the  $\eta$  feeddown from  $\eta'(958)$  decays, we introduce the 'direct' production rate  $\eta_{\text{dir}} = \eta - \text{BR}(\eta' \rightarrow \eta X) \cdot \eta'$ , where  $\text{BR}(\eta' \rightarrow \eta X) = 64.6\%$  [12]. Table 3 shows the  $\eta'(958)/\eta_{\text{dir}}$  ratios, where the  $\eta$  results have been taken from reference [17]. Within errors, the measured ratios in continuum data and direct  $\Upsilon(1S)$  decays are identical. The Lund model apparently overestimates the ratio by a factor of 2.5 in the  $\Upsilon(1S)$  and 3.2 in the continuum data. The continuum prediction of the UCLA model agrees with the measured ratio.

While the statistics in the continuum is too small to split the signal into energy intervals, this can be done for the  $\Upsilon(1S)$  data. Fig. 2 shows the  $\eta'(958)$  scaled energy spectrum on the  $\Upsilon(1S)$  resonance, where the continuum has not been subtracted, because of the statistical error; instead, the continuum admixture was accounted for in the model curves. An effective model shape was obtained by mixing shapes from continuum and  $\Upsilon(1S)$  decays in the ratio of the measured cross sections, using always the shape from Lund 7.2 for the continuum part. The lines superimposed in Fig. 2 show the model predictions with the  $\eta'(958)$  energy spectrum from direct  $\Upsilon(1S)$  decays chosen according to Lund 7.2 (broken line), and according to  $dN/dz \sim \beta e^{-10.6z}$  (solid line), as derived from the vector meson spectra. The latter curve reproduces the observed spectrum remarkably well, giving support to the extrapolation method we have used, though the spectrum obtained with the Lund  $\Upsilon(1S)$  parametrization cannot be ruled out because of limited statistics.

The  $\eta'(958)$  production has also been measured by MARK II [18] and recently by ALEPH [19, 20]. The charm decay contribution should be roughly similar in the three experiments, since the  $b \rightarrow c$  feeddown compensates the smaller  $c\bar{c}$  fraction in hadronic  $Z^0$  decays. One thus has results in  $q\bar{q}$  fragmentation for three different center-of-mass energies, displayed in table 4. The  $\eta'/\eta$  ratios obtained from ARGUS and ALEPH are quite similar, the larger ratio from MARK II being still compatible within errors. The  $\eta'(958)$  suppression relative to  $\eta$  appears to be independent of the energy scale.

## 5 Interpretation of $\eta'(958)$ Results

If one attempts to interpret the  $\eta'(958)/\eta$  production ratio based on the philosophy that the production rate of a specific meson type depends mainly on its quark content and spin, the pseudoscalar mixing angle  $\theta_P$  plays a crucial part, because it determines the mixing of the  $SU(3)$  singlet and octet pseudoscalars with isospin zero into the observable  $\eta$  and  $\eta'(958)$  mesons and thus influences their strangeness content. In the Lund and UCLA models, the two mesons are

treated as if their strangeness content is equal [2, 5], which is the case if the mixing angle is near  $\theta_P = -10^\circ$ . Direct measurements of the mixing angle [21] have however revealed a value close to  $\theta_P = -20^\circ$ , which assigns more strangeness to the  $\eta'(958)$  and less to the  $\eta$  meson. If the usual strangeness suppression factors are applied to both mesons according to their respective strangeness content, one can expect the Lund prediction for the  $\eta'/\eta_{\text{dir}}$  ratio to decrease from 0.88 to about 0.47 (we discuss only the  $\Upsilon(1S)$  case, since the charm contribution in the  $q\bar{q}$  case prevents easy scaling) [10]. A prediction by the UCLA model with accordingly modified Clebsch-Gordan coefficients is not yet available [14].

There are other effects influencing the  $\eta$  and  $\eta'(958)$  rates which are not simulated in the models, as the production of mesons with angular momentum, like scalar, pseudovector and tensor mesons. A multitude of such states populates the 900 – 1600 MeV/ $c^2$  mass range, which appear to favour strongly the  $\eta$  over the  $\eta'(958)$  decay modes [12], not unexpected regarding the limited phase space in the decay. The production of these states in fragmentation has as yet scarcely been measured, and not all of their branching ratios are known with good precision. From a more comprehensive knowledge in this sector, understanding of hadronization would clearly benefit. The  $\eta'/\eta$  system makes a good place to test such an understanding, since both particles have the same spin, thus avoiding the additional complications which arise when pseudoscalar and vector mesons are compared.

## 6 Extraction of $f_0(975)$ Rates

The  $f_0(975)$  meson is reconstructed in the  $\pi^+\pi^-$  decay channel. The mass spectrum from the  $\Upsilon(1S)$  energy is shown in fig. 3 where, besides clear peaks from  $K_S^0$  and  $\rho(770)^0$  production a signal is observed just below 1 GeV/ $c^2$ . While further  $\pi^+\pi^-$  combinations from the decays  $\eta \rightarrow \pi^+\pi^-\pi^0$ ,  $\eta'(958) \rightarrow \eta\pi^+\pi^-$  and  $\omega(783) \rightarrow \pi^+\pi^-\pi^0$  contribute only at masses below 600 MeV/ $c^2$ , the  $f_0(975)$  lies within the mass range of the broad  $\rho^0$  signal, and a reflection of the decay  $K^*(892)^0 \rightarrow K^+\pi^-$ , where the kaon is misidentified as a pion. The shape of the  $K^*$  reflection as a function of momentum is calculated from the direct  $K^*$  cross section measurement [9], and subsequently subtracted from the mass spectrum. The  $\rho^0$  signal has to be fitted simultaneously with the  $f_0(975)$  signal. The  $f_0(975)$  shape is parametrized as a relativistic s-wave Breit-Wigner function with the nominal parameters  $m_0 = 976$  MeV/ $c^2$  and  $\Gamma_0 = 34$  MeV/ $c^2$  from the particle data group [12]. The  $\rho^0$  signal is parametrized with an exponentially damped Breit-Wigner function derived from model studies [9]. To reduce combinatorial background, we subtract the same-charge  $\pi^+\pi^\pm$  spectrum before applying the fit. The different combinatorics in same-charge and opposite-charge combinations is accounted for by appropriate weighting. The remaining combinatorial background is parametrized by a second order polynomial. The fitted mass spectrum for the  $\Upsilon(1S)$  data is displayed in fig. 4.

The signal can be divided into six intervals of fractional energy  $z$  for the  $\Upsilon(1S)$ ,  $\Upsilon(2S)$  and continuum data samples. The resulting differential cross sections are summarized in tables 5 to 7. The scaled energy spectra, displayed in figs. 5 and 6, can be fitted and extrapolated with exponential functions of the type  $dN/dz \sim \beta e^{-az}$ . The fitted slope of  $a = 13.2 \pm 2.5$  for the  $\Upsilon(1S)$  data is still in agreement with the slope measured for vector mesons in table 1. The observed part of the spectrum amounts to 81% (continuum), 80% (direct  $\Upsilon(1S)$  decays) and 74% (direct  $\Upsilon(2S)$  decays) of the full yield, so that extrapolation does not play a very crucial part. The resulting  $f_0(975)$  rates per event are summarized in table 8, also given is the HRS result in the continuum at 29 GeV [22].

## 7 Discussion of $f_0(975)$ Results

The observed energy spectrum shape in continuum events is in acceptable agreement with the one measured by HRS at  $\sqrt{s} = 29$  GeV. For comparison, it is convenient to use the production rate ratio  $f_0(975)/\rho(770)^0$ , which we measure as  $0.117 \pm 0.030$  in direct  $\Upsilon(1S)$  decays and as  $0.072 \pm 0.018$  for continuum events (taking the  $\rho$  measurements from [9]). HRS obtains  $0.063 \pm 0.032$  in continuum events at 29 GeV, while the LEBE experiment has measured a ratio of  $0.059 \pm 0.021$  in soft proton-proton interactions [23].

The fact that the relative production rates of  $f_0(975)$  and  $\rho$  mesons are rather independent of the center-of-mass energy points to similar formation mechanisms for the two mesons, where only the angular momentum between the quarks in the  $f_0(975)$  case causes a suppression. The similarity of its momentum spectrum shape compared to the  $\rho(770)$  in the  $\Upsilon(1S)$  case supports this conclusion further, while the difference between continuum and  $\Upsilon(1S)$  ratios can be regarded as a hint for differing branching ratios in charm decays. While the detailed charm branching ratios into  $\rho$  and  $f_0(975)$  mesons are not sufficiently well known, it is possible to obtain inclusive information from the  $\Upsilon(4S)$  data: since more charm quarks are produced per  $B\bar{B}$  event than per continuum event, the meson multiplicities  $n_c$  from charm decays and  $n_F$  from pure fragmentation can be disentangled by comparing the meson rates in continuum and  $\Upsilon(4S)$  events. The method is described in detail in ref. [9]. The  $n_F$  results from this analysis yield a pure-fragmentation ratio of  $f_0(975)/\rho(770)^0 = 0.106 \pm 0.032$ , in good agreement with the  $\Upsilon(1S)$  result.

While these observations agree with the picture of the  $f_0(975)$  being a normal scalar meson, more exotic interpretations of this state are not excluded. One approach regards the  $f_0(975)$  as a candidate for a  $q\bar{q}q\bar{q}$  bound state [24]. Other models predict the existence of meson-like KK molecule states [25], which might be identified with the  $f_0(975)$  and the  $a_0(980)$ , a scenario supported by the mesons' small masses and widths, their large branching ratio into  $K\bar{K}$  final states and their small production cross sections in two-photon interactions [26], but contradicted by detailed investigations of the  $f_0(975)$  mass distribution [27]. As in our deuteron analysis [28], we have compared the  $f_0(975)$  energy spectrum to a simple  $K\bar{K}$  coalescence model, taking the kaon spectra from ref. [29]. This study is described in detail in ref. [9]. While the size of the cross section can be reproduced with a coalescence radius around  $P_0 = 300$  MeV/c, corresponding to a space radius of 0.6 fm, the observed spectrum appears to be harder than predicted by the coalescence model, though within the precision obtained, the latter cannot be safely excluded. It should be noted that our analysis procedure relies somewhat on the  $f_0(975)$  behaving like a "normal" resonance. If e.g. a dominant fraction of its decays lay above the  $K\bar{K}$  threshold, the procedure would have to be modified.

The observation that the  $f_0(975)$  multiplicity is about 12% of the  $\rho(770)^0$  rate in direct  $\Upsilon(1S)$  decays has not only consequences for the interpretation of the yield of pions, the main decay products in  $f_0(975)$  decays, it is also relevant for the  $\eta'/\eta$  relation, since the  $a_0(980)$ , presumably very much akin to the  $f_0(975)$ , is known to have a considerable branching fraction into  $\eta$  mesons [12]. Assuming roughly the same cross sections for these two scalar mesons, and regarding the fact that the  $a_0(980)$  is an isotriplet, it is very well possible that 10–30 % of the total  $\eta$  yield stem from  $a_0(980)$  decays. Since other tensor mesons in the mass range up to 1500 MeV decay into  $\eta$ , but for kinematical reasons hardly into  $\eta'$  mesons (e.g. the  $a_2(1320)$ ), one can expect that the visible  $\eta'/\eta$  ratio is considerably lowered by the decay contributions from  $L = 1$  mesons. Detailed measurements of  $L = 1$  meson production and their decays are therefore highly desirable.

## 8 Summary

We have measured the production of  $\eta'(958)$  and  $f_0(975)$  mesons for the first time in  $e^+e^-$  interactions in the  $\Upsilon$  energy region. The observed  $\eta'(958)$  multiplicities of  $0.034 \pm 0.010 \pm 0.004$  per continuum event and  $0.115 \pm 0.037 \pm 0.02$  per direct  $\Upsilon(1S)$  decay are by factors of six (continuum) and three (direct  $\Upsilon(1S)$  decays) smaller than the values generated by the Lund model. The discrepancy could be at least partially amended if the  $\eta$  and  $\eta'(958)$  strangeness content used in the hadronization part of the model were adjusted according to the proper value of the mixing angle  $\theta_p$ . The rate of  $f_0(975)$  production is found to be  $(7.2 \pm 1.8)\%$  (continuum) and  $(11.7 \pm 3.0)\%$  (direct  $\Upsilon(1S)$  decays) of the  $\rho(770)^0$  yield, which suggests that mesons with intrinsic angular momentum play an important part in the framework of hadronization. It is conceivable that in particular the  $\eta'/\eta$  relation is influenced by feeddown from  $L \neq 0$  meson production.

### Acknowledgements

It is a pleasure to thank U. Djuanda, E. Konrad, E. Michel, and W. Reinsch for their competent technical help in running the experiment and processing the data. We thank Dr. H. Nersisyan, B. Sarau, and the DORIS group for the excellent operation of the storage ring. The visiting groups wish to thank the DESY directorate for the support and kind hospitality extended to them.

## References

- [1] R.P. Feynman, R.D. Field, Nucl. Phys. **B136** (1978) 1.
- [2] B. Andersson *et al.*, Phys. Rep. **97** (1983) 31.
- [3] *see e.g.* H. Alhara *et al.* (TPC), Phys. Rev. Lett. **53** (1984) 2378.
- [4] H. Albrecht *et al.* (ARGUS), Phys. Lett. **B183** (1987) 419.  
H. Albrecht *et al.* (ARGUS), Z. Phys. **C39** (1988) 177.
- [5] C. D. Buchanan and S.B. Chun, UCLA-HEP-91-006.  
C. D. Buchanan and S.B. Chun, Phys. Rev. Lett. **59** (1987) 1997.
- [6] H. Albrecht *et al.* (ARGUS), Z. Phys. **C55** (1992) 25.
- [7] H. Albrecht *et al.* (ARGUS), Nucl. Instr. Meth. **A275** (1989) 1.
- [8] H. Albrecht *et al.* (ARGUS), Z. Phys. **C41** (1989) 557.
- [9] A. Lindner, Doctoral thesis Dortmund (1992), *unpublished*.
- [10] A. Zimmermann, Diploma thesis Dortmund (1992), *unpublished*.
- [11] The  $\gamma\gamma$  mass spectra resemble those in ref. [17].
- [12] Particle Data Group, Phys. Lett. **B239** (1990) 1.

## Tables

- [13] H. Albrecht *et al.* (ARGUS), Phys. Lett. **B199** (1987) 291.
- [14] C. D. Buchanan, private communication.
- [15] H. Albrecht *et al.* (ARGUS), Z. Phys. **C54** (1992) 1.  
D. Bortoletto *et al.* (CLEO), Phys. Rev. Lett. **64** (1990) 2117.
- [16] H. Albrecht *et al.* (ARGUS), Phys. Lett. **B245** (1990) 315.
- [17] H. Albrecht *et al.* (ARGUS), Z. Phys. **C46** (1990) 15.
- [18] G. Abrams *et al.* (MARK II), Phys.Rev.Lett. **61** (1988) 1057.
- [19] D. Buskulic *et al.* (ALEPH), CERN-PPE-92-074 (May 1992), submitted to Phys. Lett. **B**.  
S. Haywood (ALEPH), private communication.
- [20] Extrapolation from the ALEPH  $z > 0.1$  numbers was done using extrapolation factors by S. Haywood (ALEPH).
- [21] H. Kolanoski and P. Zerwas: "Two Photon Physics", High Energy Electron Positron Physics (eds. A. Ali and P. Söding), World Scientific (1988) 695.  
D. Williams *et al.* (Crystal Ball), Phys. Rev. **D38** (1988) 1365.  
F. Gilman and R. Kauffman, Phys. Rev. **D36** (1987) 2761.  
H. Albrecht *et al.* (ARGUS), Phys.Lett. **B199** (1987) 457.
- [22] S. Abachi *et al.* (HRS), Phys. Rev. Lett. **57** (1986) 1990.
- [23] M. Aguilar-Benitez *et al.* (LEBC-EHS), Z. Phys. **C50** (1991) 405
- [24] R.L. Jaffe, Phys. Rev. **D15** (1977) 267.  
N.N. Achasov, S.A. Devyanin and G.N. Shestakov, Phys. Lett. **B108** (1982) 134, Erratum p.435.
- [25] J. Weinstein, N. Isgur, Phys. Rev. **D41** (1990) 2236
- [26] T. Barnes, Phys. Lett. **B165** (1985) 434.
- [27] D. Morgan, M.R. Pennington, Phys. Lett. **B258** (1991) 444.
- [28] H. Albrecht *et al.* (ARGUS), Phys. Lett. **B236** (1990) 102.
- [29] H. Albrecht *et al.* (ARGUS), Z. Phys. **C44** (1989) 547.

| Meson type       | Slope parameter <sup>a</sup> |
|------------------|------------------------------|
| $K^*(892)^+$     | $10.74 \pm 0.84$             |
| $K^*(892)^0$     | $10.49 \pm 0.29$             |
| $\rho(770)^0$    | $10.17 \pm 0.72$             |
| $\omega(783)$    | $10.75 \pm 1.36$             |
| Weighted average | 10.60                        |

Table 1: Values determined for slope parameter  $a$  from vector meson  $z$  spectra in direct  $\Upsilon(1S)$  decays, taken from ref. [9]

| Data type      | $\sqrt{s}$ [GeV] | $\eta_{\eta'}$<br>$z > 0.35$ | $\eta_{\eta'}$<br>total     | $\eta_{\eta'}$ | $\eta_{\eta'}$ |
|----------------|------------------|------------------------------|-----------------------------|----------------|----------------|
|                |                  |                              |                             | Lund 7.2       | UCLA           |
| Continuum      | 9.36-10.45       | $0.014 \pm 0.006$            | $0.034 \pm 0.010 \pm 0.004$ | 0.194          | 0.08           |
| $\Upsilon(1S)$ | 9.46             | $0.034 \pm 0.011$            | $0.115 \pm 0.037 \pm 0.02$  | 0.32           | —              |
| $\Upsilon(2S)$ | 10.02            | —                            | $0.12 \pm 0.08 \pm 0.02$    | 0.33           | —              |
| $\Upsilon(4S)$ | 10.58            | —                            | $< 0.30$ (90%C.L.)          | —              | —              |

Table 2: The direct  $\eta'(958)$  rates per event. The total rates rely on the momentum spectra as given by Lund 7.2, except in the  $\Upsilon(1S)$  case, where the  $z > 0.35$  values were extrapolated with the function  $\beta e^{-10.6z}$  (see text).

| Data type      | $\eta$<br>[17]  | $\eta'/\eta_{dir}$ | $\eta'/\eta_{dir}$ |
|----------------|-----------------|--------------------|--------------------|
|                |                 | Lund 7.2           | UCLA               |
| $\Upsilon(1S)$ | $0.40 \pm 0.17$ | $0.35 \pm 0.24$    | 0.88               |
| Continuum      | $0.19 \pm 0.06$ | $0.20 \pm 0.10$    | 0.24               |

Table 3: The ratio  $\eta'(958) / \eta_{dir}$ , with  $\eta_{dir} = \eta - BR(\eta' \rightarrow \eta X) \cdot \eta$ .

| Meson            | ARGUS                       | MARK II                     | ALEPH                       |
|------------------|-----------------------------|-----------------------------|-----------------------------|
|                  | $\sqrt{s} = 10 \text{ GeV}$ | $\sqrt{s} = 29 \text{ GeV}$ | $\sqrt{s} = 90 \text{ GeV}$ |
| $\eta$           | $0.19 \pm 0.06$             | $0.60 \pm 0.08$             | $0.298 \pm 0.031$           |
| $\eta'(958)$     | $0.034 \pm 0.011$           | $0.26 \pm 0.10$             | $0.068 \pm 0.024$           |
| $\eta(958)/\eta$ | $0.18 \pm 0.08$             | $0.43 \pm 0.18$             | $0.24 \pm 0.09$             |
|                  |                             |                             | total [20]                  |
|                  |                             |                             | $z > 0.1$                   |
|                  |                             |                             | $1.11 \pm 0.17$             |
|                  |                             |                             | $0.165 \pm 0.058$           |
|                  |                             |                             | $0.15 \pm 0.06$             |

Table 4:  $\eta$  and  $\eta'(958)$  production rates in  $q\bar{q}$  final states for three different center-of-mass energies. The numbers for  $z > 0$  have been obtained by extrapolating the  $z > 0.1$  numbers with extrapolation factors based on the Lund model [20].

| z range     | $1/(\beta\sigma_{q\bar{q}}^0) \cdot d\sigma^0/dz$ | z range     | $1/(\beta\sigma_{q\bar{q}}^0) \cdot d\sigma^0/dz$ |
|-------------|---|-------------|---|
| 0.230-0.275 | $0.313 \pm 0.090 \pm 0.037$                       | 0.464-0.611 | $0.0108 \pm 0.0069 \pm 0.0013$                    |
| 0.275-0.368 | $0.065 \pm 0.028 \pm 0.008$                       | 0.611-0.709 | $0.0087 \pm 0.0047 \pm 0.0010$                    |
| 0.368-0.464 | $0.029 \pm 0.015 \pm 0.003$                       | 0.709-1.000 | $-0.0004 \pm 0.0014 \pm 0.0001$                   |

Table 5: Radiation-corrected normalized cross section  $1/(\beta\sigma_{q\bar{q}}^0) \cdot d\sigma^0/dz$  for  $f_0(975)$  production in continuum events.

| z range     | $1/(\beta\sigma_{\text{dir}}) \cdot d\sigma/dz$ | z range     | $1/(\beta\sigma_{\text{dir}}) \cdot d\sigma/dz$ |
|-------------|---|-------------|---|
| 0.237-0.280 | $0.41 \pm 0.20 \pm 0.05$                        | 0.467-0.613 | $0.006 \pm 0.010 \pm 0.001$                     |
| 0.280-0.372 | $0.181 \pm 0.056 \pm 0.023$                     | 0.613-0.711 | $-0.0074 \pm 0.0052 \pm 0.0009$                 |
| 0.372-0.467 | $0.087 \pm 0.025 \pm 0.011$                     | 0.711-1.000 | $0.0016 \pm 0.0012 \pm 0.0002$                  |

Table 6: Normalized cross section  $1/(\beta\sigma_{\text{dir}}) \cdot d\sigma/dz$  for  $f_0(975)$  production in direct  $\Upsilon(1S)$  decays.

| z range     | $1/(\beta\sigma_{\text{dir}}) \cdot d\sigma/dz$ | z range     | $1/(\beta\sigma_{\text{dir}}) \cdot d\sigma/dz$ |
|-------------|---|-------------|---|
| 0.233-0.277 | $0.28 \pm 0.29 \pm 0.04$                        | 0.466-0.612 | $-0.001 \pm 0.022 \pm 0.0001$                   |
| 0.277-0.370 | $0.222 \pm 0.087 \pm 0.028$                     | 0.612-0.710 | $0.002 \pm 0.011 \pm 0.0003$                    |
| 0.370-0.466 | $0.013 \pm 0.041 \pm 0.002$                     | 0.710-1.000 | $0.0005 \pm 0.0026 \pm 0.0001$                  |

Table 7: Normalized  $f_0(975)$  cross section  $1/(\beta\sigma_{\text{dir}}) \cdot d\sigma/dz$  for  $f_0(975)$  production in direct  $\Upsilon(2S)$  decays.

| Data type      | $\sqrt{s}$ [GeV] | $n(f_0(975))$ this expt.       | $\sqrt{s}$ [GeV] | $n(f_0(975))$ HRS [22] |
|----------------|------------------|--------------------------------|------------------|------------------------|
| Continuum      | 10.45            | $0.0236 \pm 0.0047 \pm 0.0033$ | 29               | $0.11 \pm 0.04$        |
| $\Upsilon(1S)$ | 9.46             | $0.0390 \pm 0.0088 \pm 0.0049$ | —                | —                      |
| $\Upsilon(2S)$ | 10.02            | $0.0350 \pm 0.0156 \pm 0.0045$ | —                | —                      |
| $\Upsilon(4S)$ | 10.58            | $< 0.050$ (90 % C.L.)          | —                | —                      |

Table 8: The direct  $f_0(975)$  production rates per event. Also shown are results from the HRS group, taken in the continuum at 29 GeV.



## Figure Captions

Figure 1 Invariant  $\eta\pi^+\pi^-$  mass spectra in data taken (a) at the  $\Upsilon(1S)$  resonance energy, (b) at the  $\Upsilon(2S)$  resonance energy, (c) at the  $\Upsilon(4S)$  resonance energy and (d) in the  $q\bar{q}$  continuum. The curves display fits with a Gaussian parametrization for the signal, with mass and width taken from Monte Carlo, plus a 4<sup>th</sup> order polynomial background function.

Figure 2 Inclusive  $z$  spectrum of  $\eta'(958)$  mesons at the  $\Upsilon(1S)$  resonance energy, underlying continuum *not* subtracted. The dashed line is the Lund spectrum for  $\Upsilon(1S)$  decays plus underlying continuum, both normalized to the measured multiplicities. For the solid line, the direct  $\Upsilon(1S)$  part is modelled with the shape from the vector meson spectra.

Figure 3 Invariant  $\pi^+\pi^-\pi^-$  mass spectrum for  $z(\pi^+\pi^-) > 0.2$  in data taken at the  $\Upsilon(1S)$  energy.

Figure 4 Invariant  $\pi^+\pi^-\pi^-$  mass spectrum for  $z(\pi^+\pi^-) > 0.2$  after subtraction of the same-charge ( $\pi^\pm\pi^\pm$ ) distribution and the  $K^*(892)^0$  reflection in data taken at the  $\Upsilon(1S)$  energy. The superimposed lines are the fits described in the text, with and without the  $\rho(770)^0$  contribution.

Figure 5 Scaled energy spectrum for  $f_0(975)$  mesons in direct decays of the  $\Upsilon(1S)$  resonance. The line represents the fitted exponential which was used for extrapolation.

Figure 6 Scaled energy spectrum for  $f_0(975)$  mesons in nonresonant continuum events near  $\sqrt{s} = 10.45$  GeV (full circles), and the corresponding result from HRS [22] at  $\sqrt{s} = 29$  GeV (open circles).

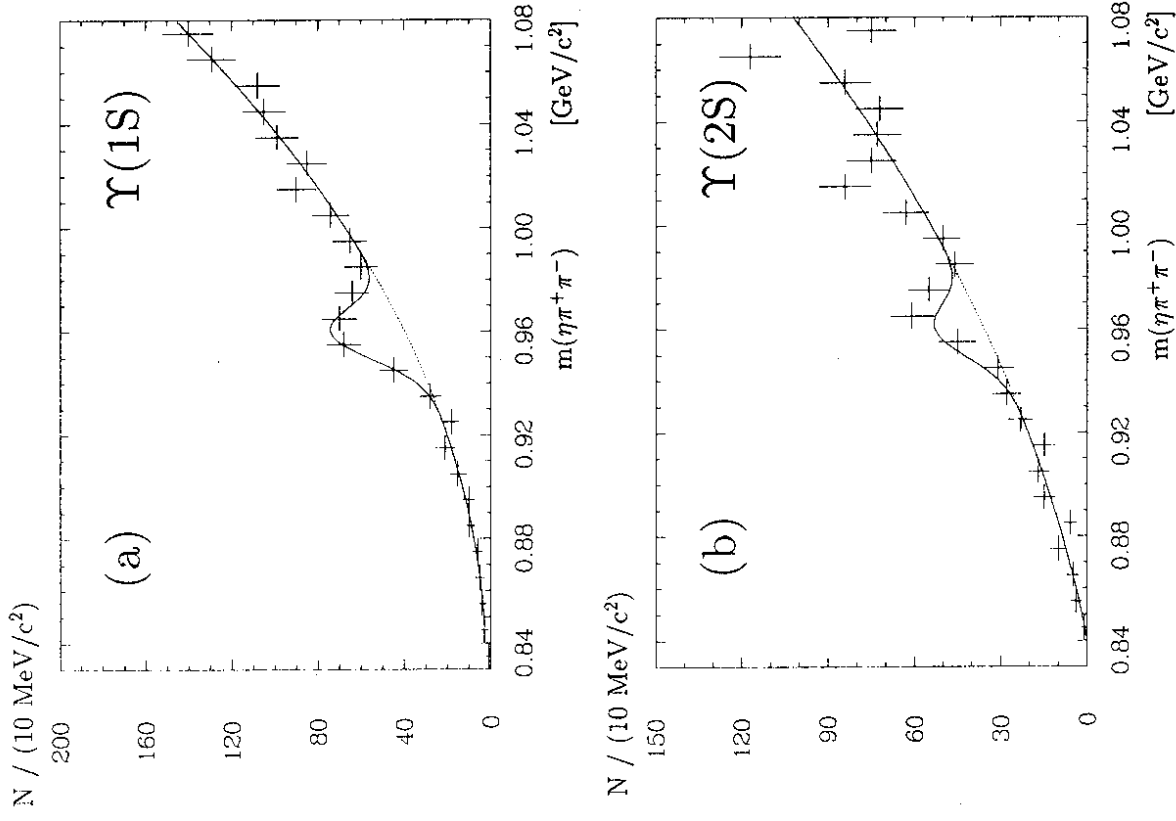


Figure 1

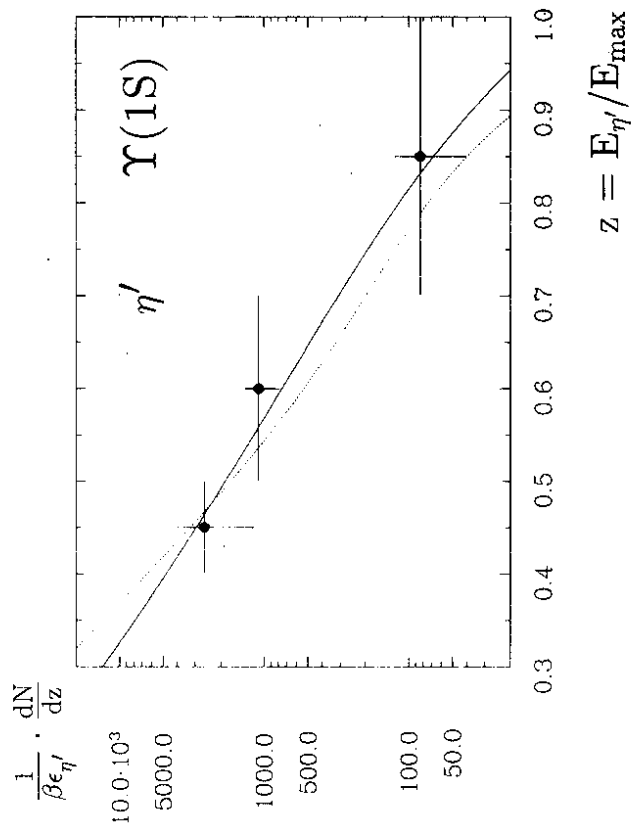
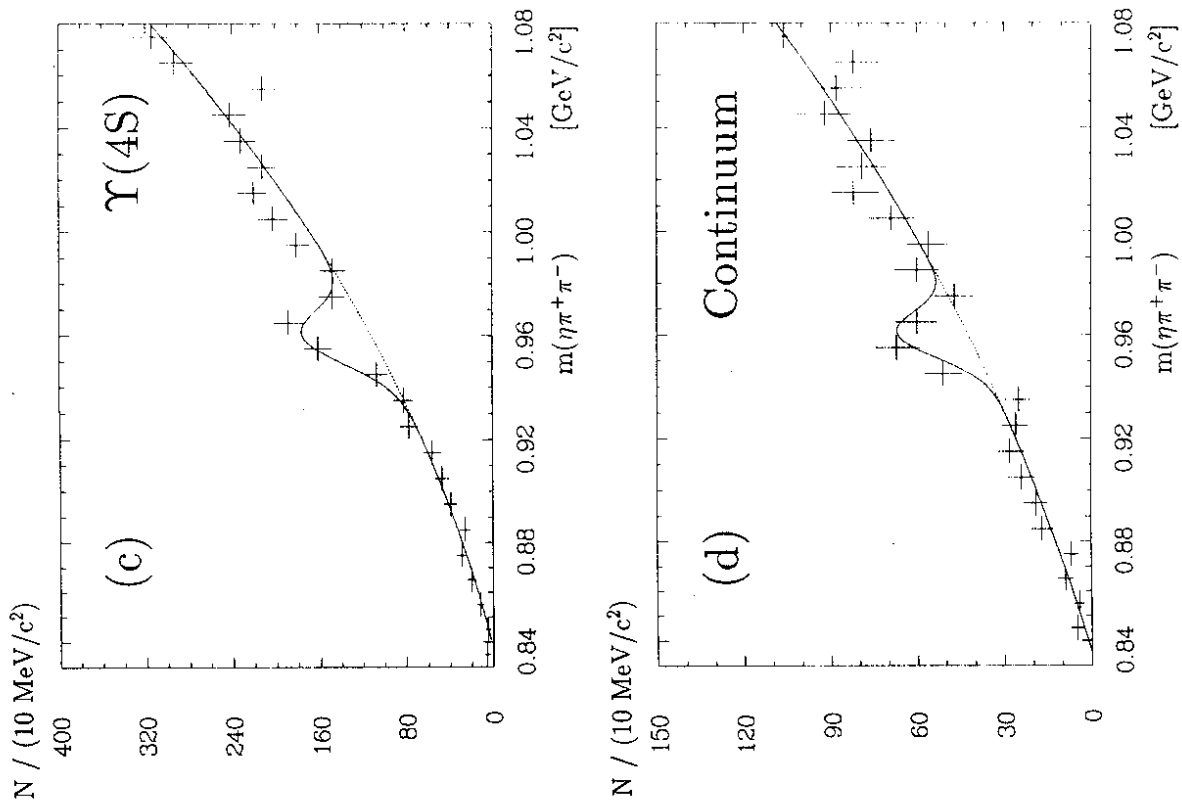


Figure 2

Figure 1 (cont'd)

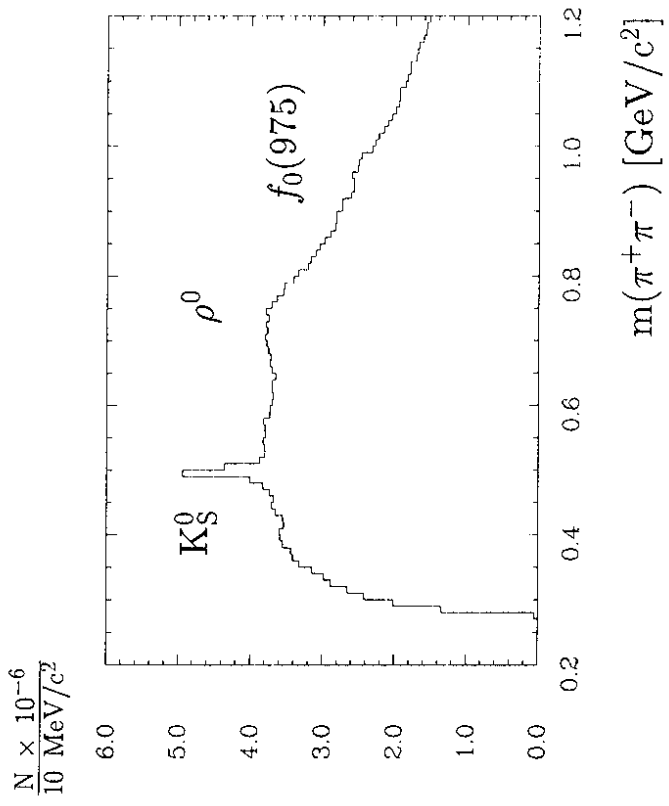


Figure 3

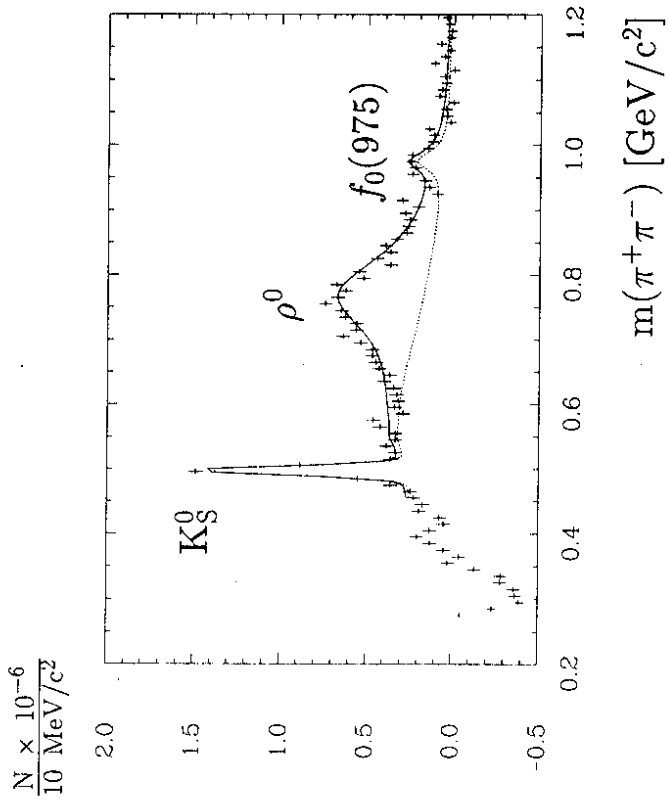


Figure 4

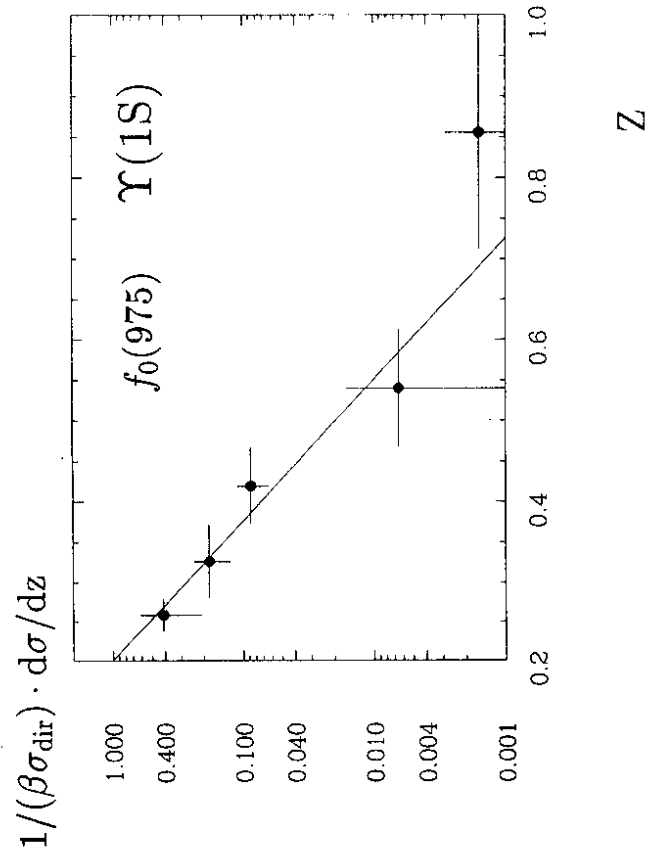


Figure 5

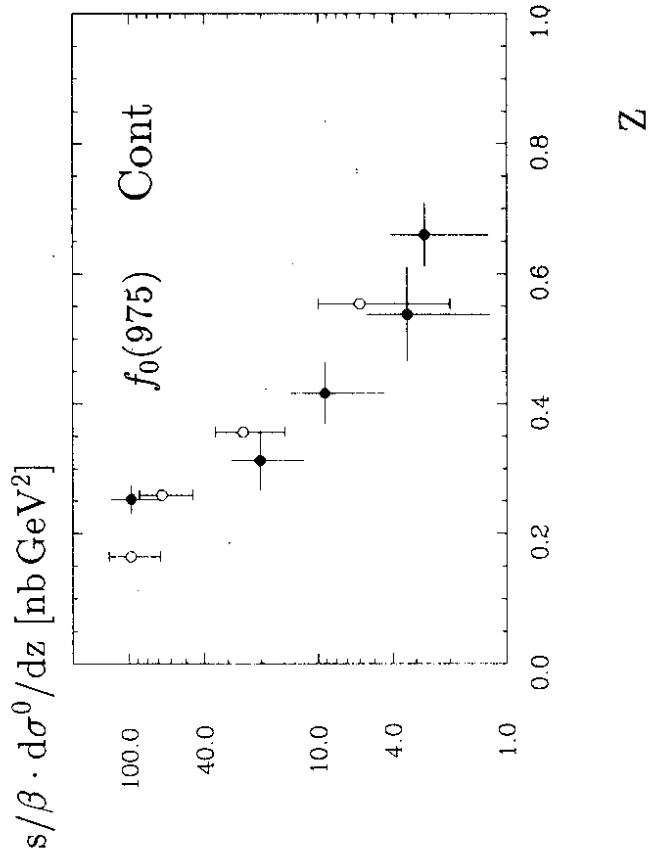


Figure 6